

## Supporting Information

### Binding Kinetics versus Affinities in BRD4 Inhibition

Ming Kuang<sup>1,2</sup>, Jingwei Zhou<sup>2</sup>, Laiyou Wang<sup>1</sup>, Zhihong Liu<sup>2</sup>, Jiao Guo<sup>1,\*</sup>, and Ruibo

Wu<sup>2,\*</sup>

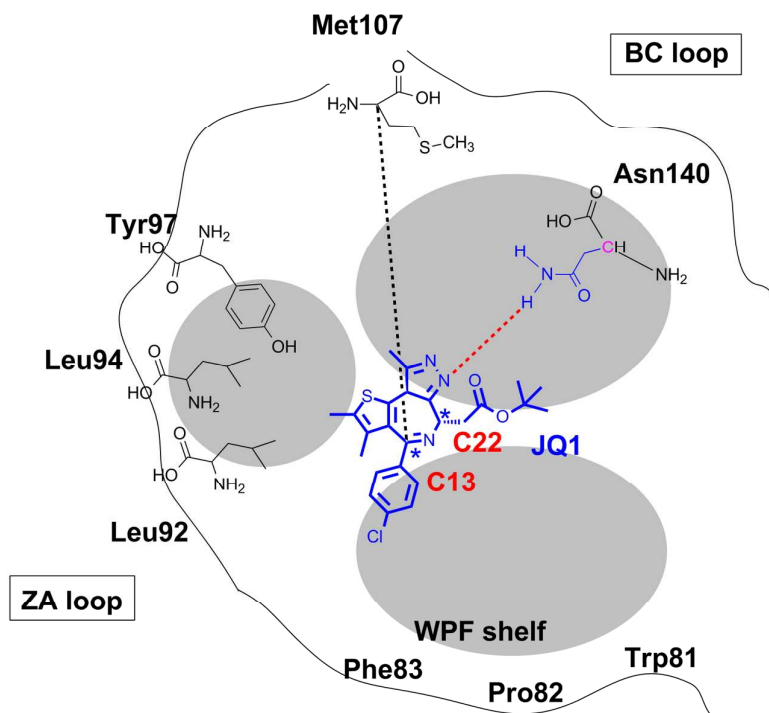
<sup>1</sup>*Guangdong Metabolic Diseases Research Center of Integrated Chinese and Western Medicine, Guangdong TCM Key Laboratory against Metabolic Diseases, Institute of Chinese Medical Sciences, Guangdong Pharmaceutical University, Guangzhou 510006, P.R. China*

<sup>2</sup>*School of Pharmaceutical Sciences, Sun Yat-sen University, Guangzhou 510006, P.R. China*

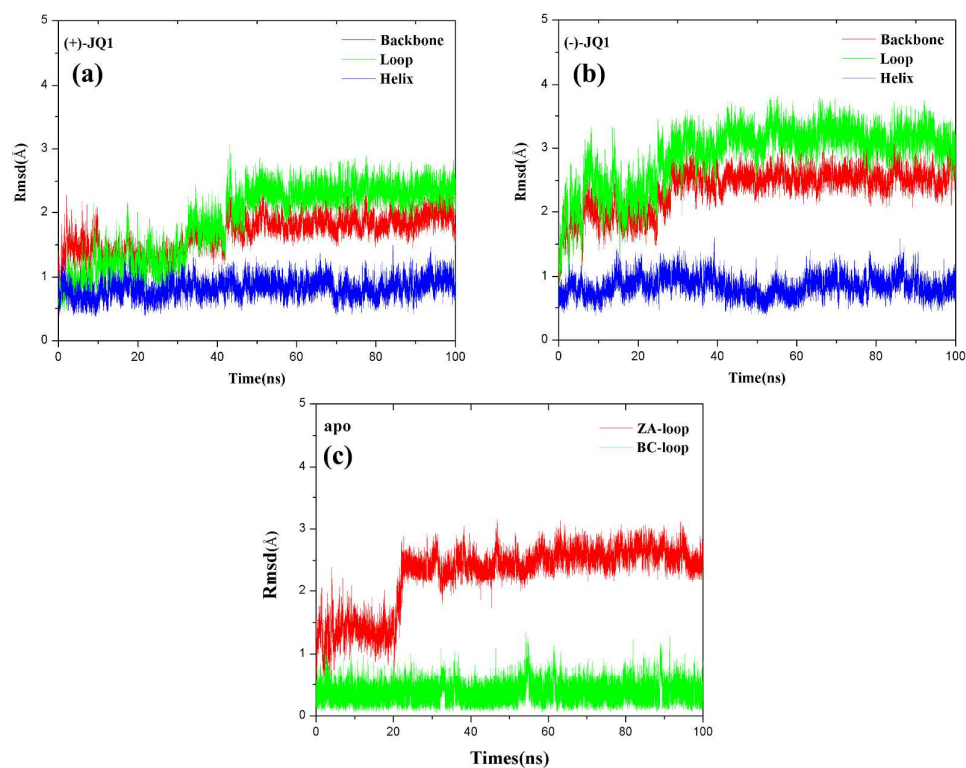
\*To whom correspondence should be addressed.

E-mail: [jiaoguo\\_gdpu@hotmail.com](mailto:jiaoguo_gdpu@hotmail.com); [wurb3@mail.sysu.edu.cn](mailto:wurb3@mail.sysu.edu.cn);

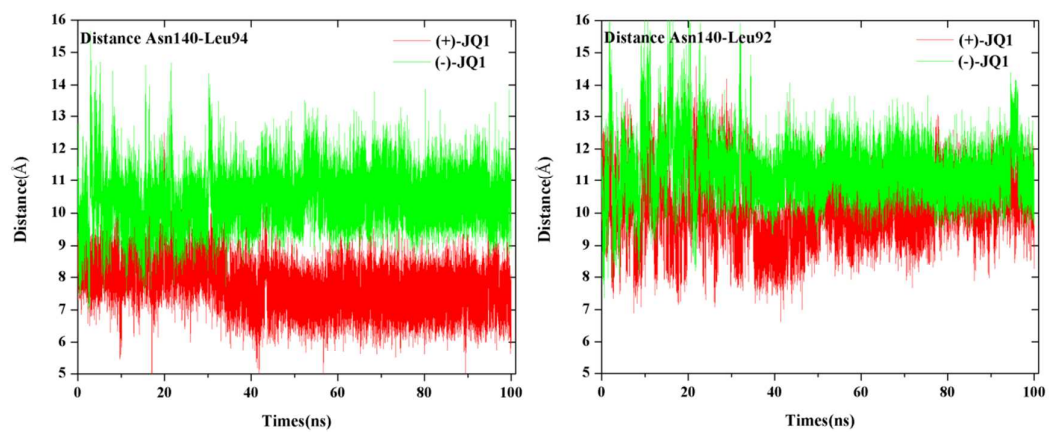
**Figure S1-S10.**



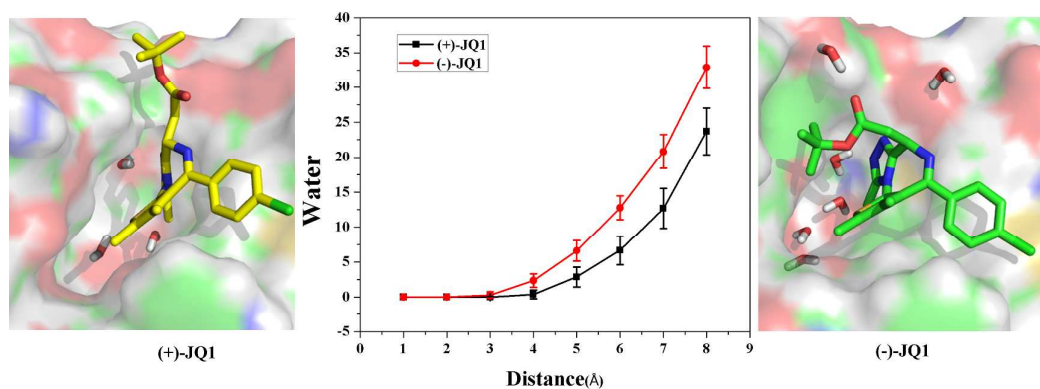
**Figure S1.** Illustration of the key residues around the (+)-JQ1 in the active pocket. The conserved and key hydrogen bond between Asn140 and ligand is shown in red dashed line. The C22 is the chiral center as noted by blue asterisk. The distance between MET107:Cα and (+)-JQ1:C13 atoms is chosen as the reaction coordinate to drive the ligand releasing process, as linked by the black dashed line. The atoms in QM region are highlighted in blue and pink (for *pseudo*-atoms).



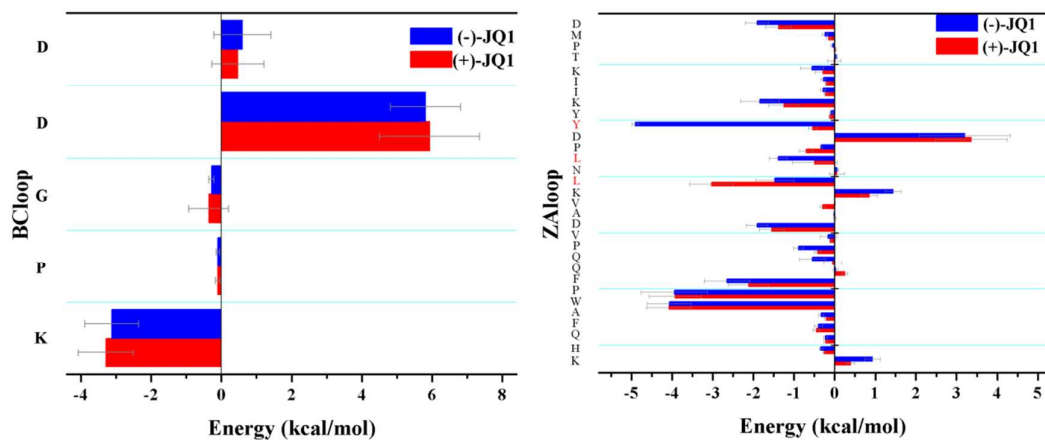
**Figure S2.** Time series of the skeleton-atoms RMSD for BRD4 in different binding states. (a) Time series of the skeleton-atoms RMSD for BRD4 with (+)-JQ1. (b) Time series of the skeleton-atoms RMSD for BRD4 with (-)-JQ1. (c) Time series of the skeleton-atoms RMSD of ZA-loop and BC-loop for BRD4 in the *apo*-state.



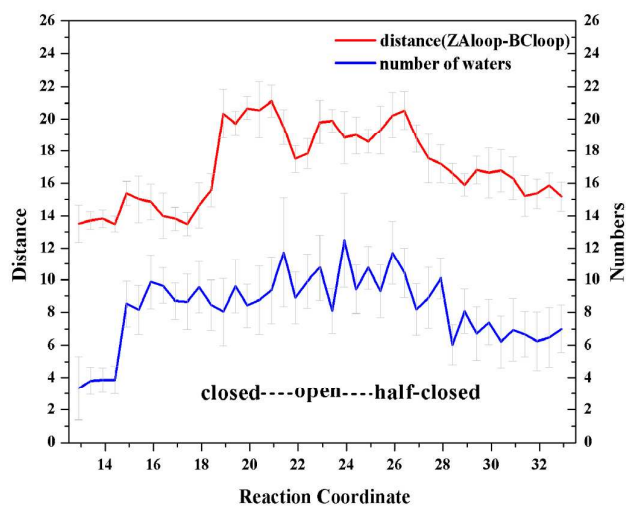
**Figure S3.** The detailed distance evolution between Asn140:C $\alpha$  and Leu94/Leu92:C $\alpha$  .



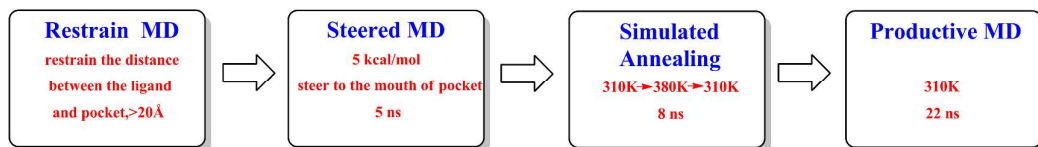
**Figure S4.** Analysis of water number around chiral carbon of JQ1 in the binding pocket.



**Figure S5.** Interaction energy analysis between ligand and residues in BC-loop and ZA-loop on the basis of the QM/MM trajectories. Residues from bottom to top refer to residues 141-145 in BC-loop (left) and residues 76-106 in ZA-loop (right). All interaction energies are calculated based on 5000 snapshots from the equilibrium QM/MM MD trajectories, and the gray error bars represent the statistical error.

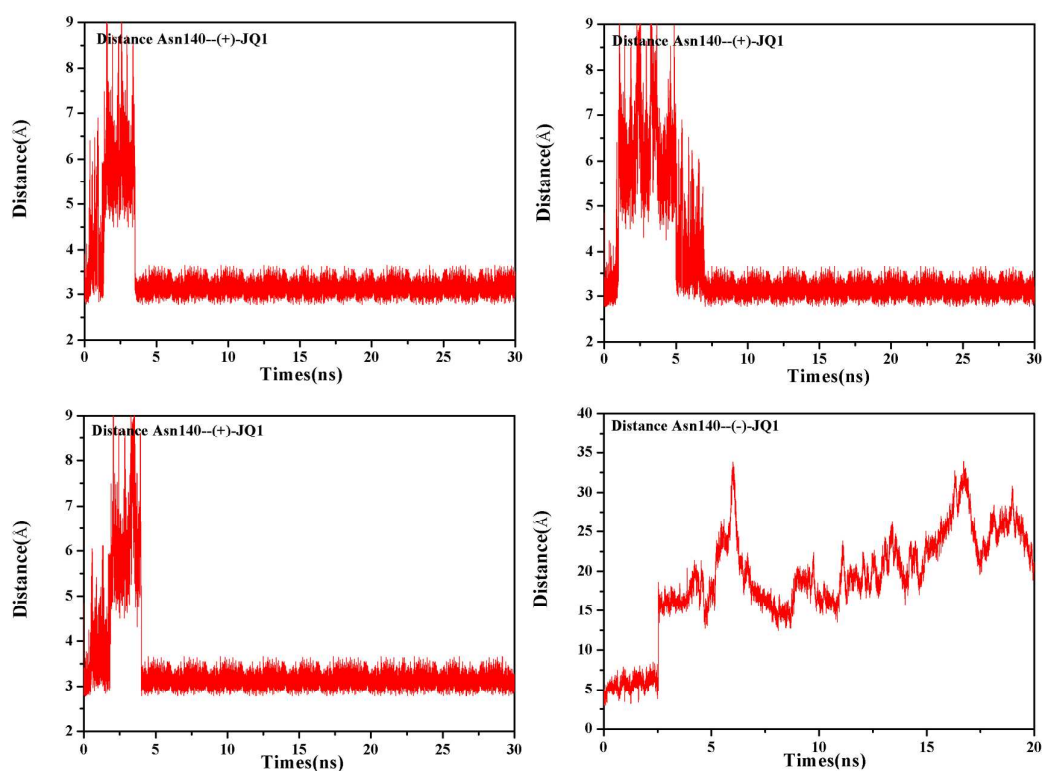


**Figure S6.** The water number and defined distance evolution along the releasing procedure of (+)-JQ1. The distance is simply defined between N140:C $\alpha$  and L94:C $\alpha$ . The 8 Å water shell center at C136: C $\alpha$  are defined to account the water molecules.

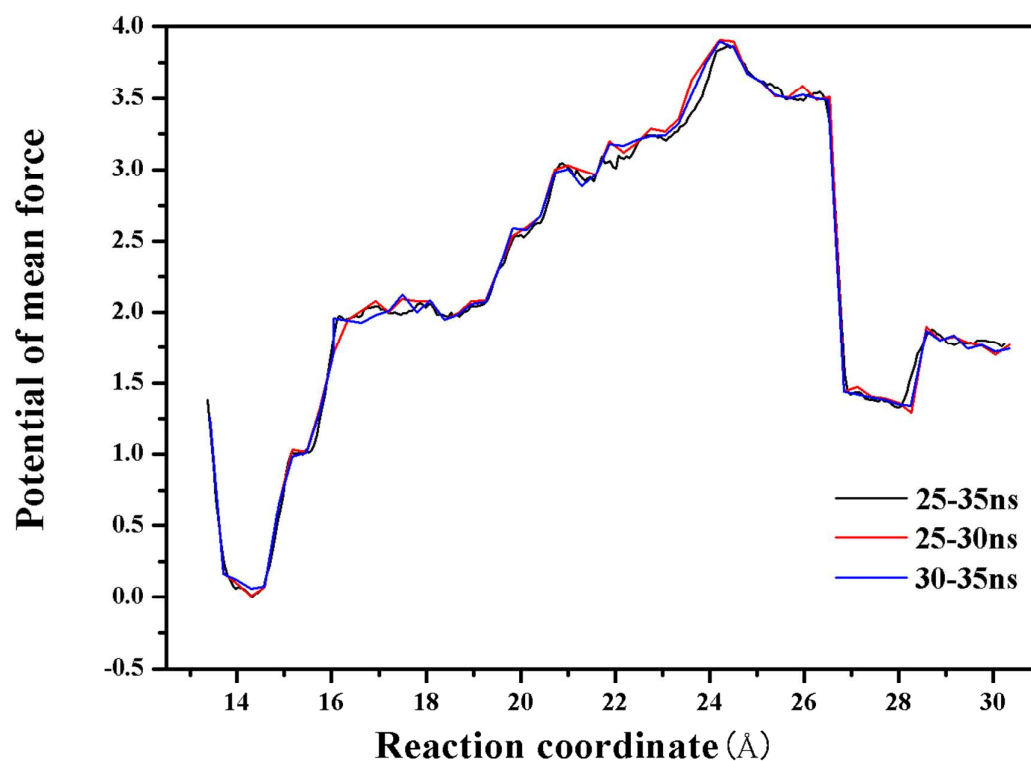


**Figure S7.** The flow chart of the steered molecular dynamics simulations to trigger the JQ1 ligands binding into BRD4 and the simulated annealing to identify the final equilibrium state. In methodology, the distance between the (+)-JQ1/(-)-JQ1 and pocket was first restraint more than 20 Å, respectively. That is, the ligands are solvated in the water solution. And the entire system was optimized and equilibrated before the steered MD simulation. Then, we employed Steered MD to steer the JQ1 ligands to the mouth of pocket with a series of biasing harmonic potential (5 kcal/mol). At the simulated annealing step, the temperature was raised up from 310K to 380K, and then cooling by reducing 10K at a time and back to 310K. The last 30 ns (8 ns simulated annealing and 22 ns productive MD) trajectories are analyzed as shown in Figure S8 and Figure 9.

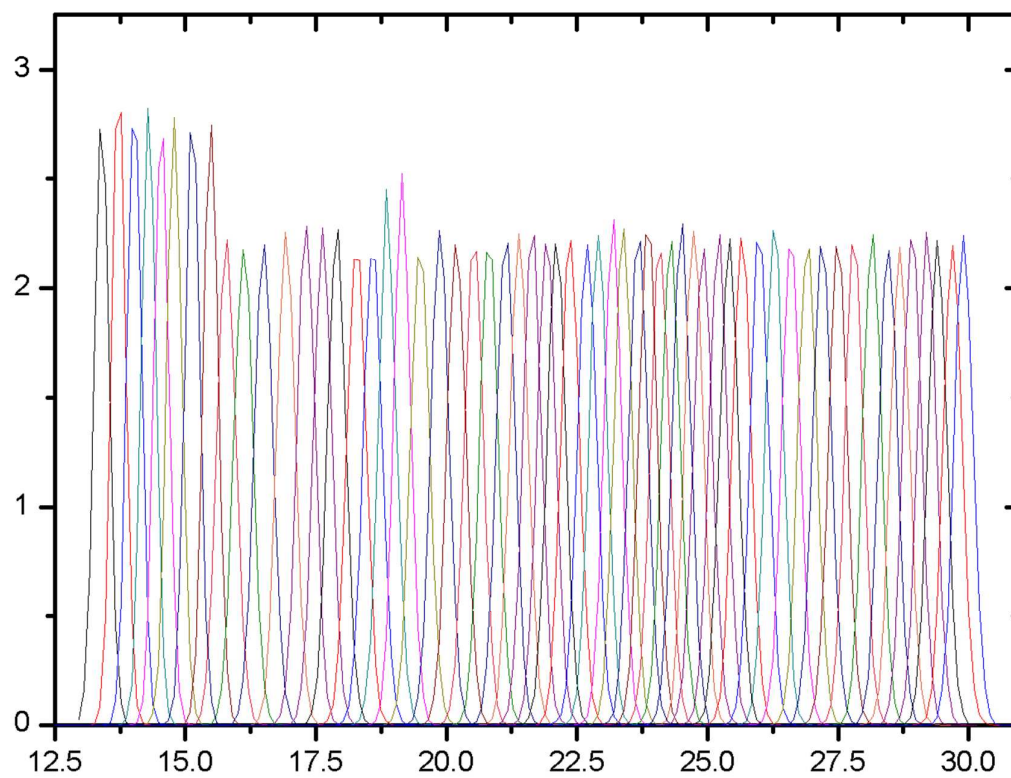




**Figure S8.** The representative distance evolution between Asn140:N and JQ1:N (the conserved strong hydrogen bond (HB) heavy-atom between N140 and JQ1, see Figure S1.) The previous three figures reveal the spontaneously binding kinetics for (+)-JQ1 successfully entering into the binding sites (four times in total among the 20 independent MD trajectories, 3 shown here and 1 shown in Figure 9). The last one represents the spontaneously binding kinetics for (-)-JQ1 reversed immigrating into the solvent in several trajectories among the 20 independent MD trajectories (see detailed MD protocol in Figure S7), otherwise, the (-)-JQ1 will maintain at the mouth of the active pocket (namely a metastable binding state) as show in Figure 9 and 10c.

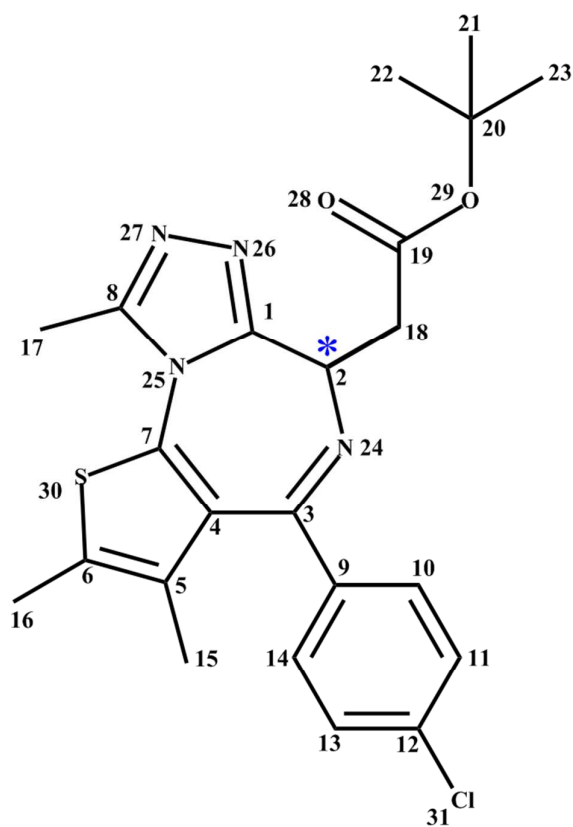


**Figure S9.** The potential of mean force profiles along the defined reaction coordinate on the basis of different trajectory range. The convergence of PMF profiles is reliable as the difference among the different time windows is very small. The ligand release experiences an average free energy barrier of  $\sim 3.8$  kcal/mol with an average endothermic of  $\sim 1.8$  kcal/mol. The benchmark test for the overlap pictures among all simulation windows are provided in Figure S10.



**Figure S10.** The overlap between neighboring windows along the defined reaction coordinate. All time windows are selected from the last 10 ns trajectory.

**Table S1.** The atomic RESP charge used in MM MD simulations (estimated at the HF/6-31G\* level).



Atom Type	Charge	
	(+)-JQ1	(-)-JQ1
C1	0.185	0.060
C2	0.414	0.485
C3	0.355	0.490
C4	0.080	-0.067
C5	-0.093	0.131
C6	0.180	0.104
C7	-0.377	-0.455
C8	0.479	0.326
C9	0.012	-0.031
C10	-0.135	-0.158
C11	-0.063	-0.059
C12	-0.021	-0.009
C13	-0.052	-0.080
C14	-0.186	-0.129
C15	-0.208	-0.405
C16	-0.523	-0.492
C17	-0.516	-0.428
C18	-0.740	-0.222
C19	1.011	0.760
C20	0.761	0.886
C21	-0.587	-0.596
C22	-0.561	-0.563
C23	-0.492	-0.431
N24	-0.541	-0.685
N25	0.219	0.470
N26	-0.277	-0.306
N27	-0.447	-0.404
O28	-0.643	-0.622
O29	-0.548	-0.612
S30	-0.029	0.024
Cl31	-0.100	-0.102